GEOLOGY | THE GEOLOGICAL SOCIETY OF AMERICA®

https://doi.org/10.1130/G47210.1

Manuscript received 15 November 2019
Revised manuscript received 5 February 2020
Manuscript accepted 10 February 2020

Radiocarbon dating supports bivalve-fish age coupling along a bathymetric gradient in high-resolution paleoenvironmental studies

Paolo G. Albano[1], Quan Hua[2], Darrell S. Kaufman[3], Adam Tomašových[4], Martin Zuschin[1] and Konstantina Agiadi[5]
[1]Department of Palaeontology, University of Vienna, 1090 Vienna, Austria
[2]Australian Nuclear Science and Technology Organisation, Kirrawee DC, NSW 2232, Australia
[3]School of Earth and Sustainability, Northern Arizona University, Flagstaff, Arizona 86011, USA
[4]Earth Science Institute, Slovak Academy of Sciences, 840 05 Bratislava, Slovak Republic
[5]Faculty of Geology and Geoenvironment, National and Kapodistrian University of Athens, Athens, Greece

ABSTRACT

Studies of paleocommunities and trophic webs assume that multispecies assemblages consist of species that coexisted in the same habitat over the duration of time averaging. However, even species with similar durability can differ in age within a single fossil assemblage. Here, we tested whether skeletal remains of different phyla and trophic guilds, the most abundant infaunal bivalve shells and nektobenthic fish otoliths, differed in radiocarbon age in surficial sediments along a depth gradient from 10 to 40 m on the warm-temperate Israeli shelf, and we modeled their dynamics of taphonomic loss. We found that, in spite of the higher potential of fishes for out-of-habitat transport after death, differences in age structure within depths were smaller by almost an order of magnitude than differences between depths. Shell and otolith assemblages underwent depth-specific burial pathways independent of taxon identity, generating death assemblages with comparable time averaging, and supporting the assumption of temporal and spatial co-occurrence of mollusks and fishes.

INTRODUCTION

Paleoecological inferences about co-occurrence patterns and niche overlap assume that species present in the same sedimentary layer are of similar age and therefore potentially interacted with each other (Lyons et al., 2016). However, fossils preserved together within a single stratum can represent organisms that lived at vastly different times due to condensation, bioturbational mixing, and physical reworking (Kowalewski, 1996; Kidwell, 2013). Multiple examples of co-occurring shells of mollusks and brachiopods have been shown to differ significantly in median ages and time averaging (Kosnik et al., 2009, 2013; Krause et al., 2010; Tomašových et al., 2014, 2019). Such differences can be generated by intrinsic factors like between-species variation in skeletal durability (Kosnik et al., 2007; Kowalewski et al., 2018), in timing and duration of shell production (Tomašových et al., 2016), or in propensity to out-of-habitat transport. These intrinsic factors can be modulated or overwhelmed by gradients in extrinsic factors that influence burial and disintegration, such as sedimentation rates (Krause et al., 2010) and pore-water chemistry (Best et al., 2007).

Although paleoecological analyses are increasingly focused on whole ecosystems (Villéger et al., 2011; Roopnarine and Angielczyk, 2015), no studies have assessed time averaging of co-occurring species belonging to phyla with different ecosystem functions. Here, we quantified time averaging and modeled disintegration and burial of suspension-feeding bivalve shells and predatory nektobenthic fish otoliths along a 10–40 m depth gradient on the Mediterranean Israeli shelf to test the hypothesis that species co-occurring in the same death assemblage but subject to different intrinsic factors did not temporally co-occur in the original biological community. The shells and otoliths of our target species have comparable size and durability, but undergo different pathways after death. Infaunal bivalves are more likely to die and be buried *in situ*. In contrast, otoliths can be deposited far from the life location because they either originate from predated fish through feces (Nolf, 1995), implying that their final location depends on the predator range, or carcasses are made buoyant by bacterial decay gases and transported to the surface where they drift away (Elder and Smith, 1988), especially at temperatures greater than 16 °C (year-round in most temperate to tropical seas). Suspension-feeding bivalves and predatory fishes can further respond differently in terms of their population fluctuations to variation in environmental factors such as nutrient regimes due, e.g., to top-down controls of the trophic web. These differences can generate major variation in the structure of time averaging (determined by median ages and indicators of age range). In contrast to our expectation, we found that both taxa possessed very similar median ages and interquartile age ranges and that differences in age structure were smaller within depths than between depths. These results suggest that mollusks and fishes co-occurred temporally and spatially, and they point to the prevalence of depth-specific taphonomic and burial pathways independent of taxon identity.

MATERIAL AND METHODS

Study Area and Target Species

We collected death assemblages with a Van Veen grab sampler at 10, 30, and 40 m depth off Ashqelon (southern Israel), Eastern Mediterranean, in autumn 2016 (Table DR1 in the GSA Data Repository[1]; Fig. 1). This is an open shelf under the sedimentary input of

[1]GSA Data Repository item 2020173, details on methods and radiocarbon ages, is available online at http://www.geosociety.org/datarepository/2020/, or on request from editing@geosociety.org.

CITATION: Albano, P.G., et al., 2020, Radiocarbon dating supports bivalve-fish age coupling along a bathymetric gradient in high-resolution paleoenvironmental studies: Geology, v. 48, p. , https://doi.org/10.1130/G47210.1

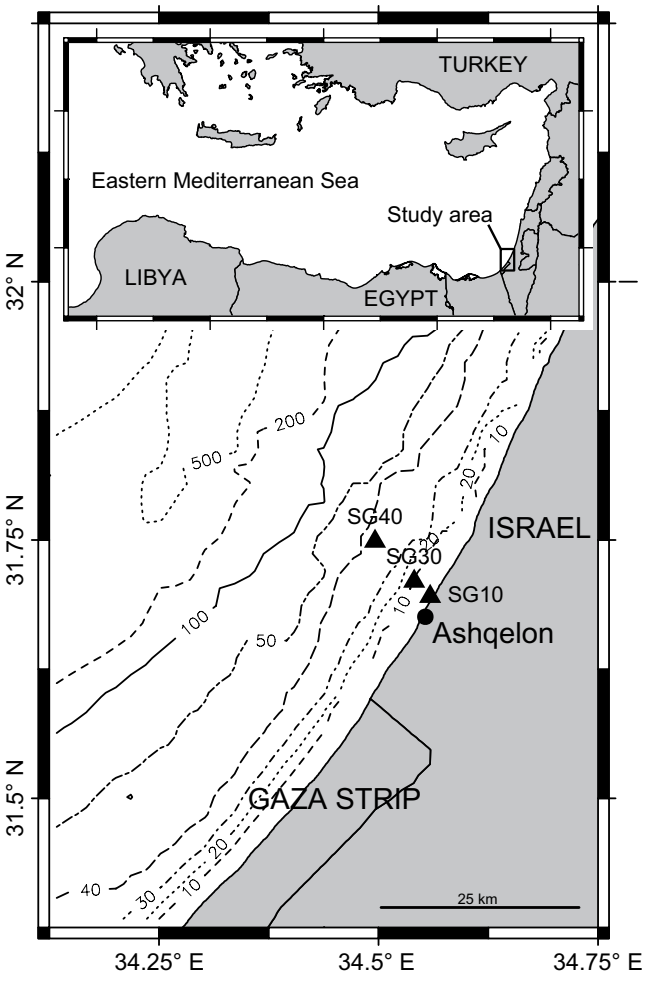

Figure 1. Map of the Levantine Basin, easternmost Mediterranean Sea, with location of three collection sites off Ashqelon, southern Israel. Depth contours in m.

the Nile River (Inman and Jenkins, 1984) and with seawater temperature between 17 °C and 30 °C. The fair weather wave base at 15–25 m (Hyams-Kaphzan et al., 2008) and strong wave-induced counterclockwise longshore currents that reach ~35 m depth transport siliciclastic sands from the Nile Delta northwards (Golik, 1993; Avnaim-Katav et al., 2015) and limit the deposition of fine-grained sediments. This bathymetric gradient thus coincides with a decline in the exposure to wave- and current-driven erosion and reworking, leading to a decline in grain size from sands to muddy sands up to muds and to a higher net sedimentation rate (2.4 mm/yr at 40 m, exceeding the rates at 10 m [0.4 mm/yr] and 30 m [0.2 mm/yr]; Goodman-Tchernov et al. [2009] and our own unpublished data based on sediment cores at the two deepest sites). We dated the bivalve *Donax semistriatus* and the benthic fish *Ariosoma balearicum* (conger eel) at 10 m, and the bivalve *Corbula gibba* and a multispecies gobiid assemblage at 30 and 40 m (Table DR2). The targeted shells and otoliths are aragonitic (Degens et al., 1969). Although *Corbula* has conchiolin layers, which retard shell dissolution in waters undersaturated in calcium carbonate and increase shell strength, its taphonomic pathway does not differ from bivalves with shell structure similar to *Donax* (Gallmetzer et al., 2019). *Corbula* and *Donax* ranged in length from 2.5 to 5.6 mm (median 3.7 mm) and from 3.0 to 16.0 mm (median 5.0 mm), respectively. Otoliths ranged in length from 1.5 to 7.5 mm (median 3.5 mm). Their taphonomic pathways are poorly known, but otoliths are regarded as durable remains (Nolf, 1985).

Shell and Otolith Dating

Shells and otoliths were dated by accelerator mass spectrometry (AMS), using powdered carbonate targets (Bush et al., 2013). Four shells were also analyzed using the standard graphite-target method to assess the accuracy of carbonate targets, but we did not conduct such an assessment for otoliths due to their small size. Shell carbonate-target ages had a small offset for the youngest samples (Table DR6). However, we used the measured carbonate-target ages for both types of samples because a correction for the offset did not change our results (see the Data Repository and Table DR7). Radiocarbon ages were converted to calendar ages (see the Data Repository). We report all ages in calendar years before 2016 CE, the year of sample collection.

Age-Frequency Distributions

We computed measures of central tendency (median age), dispersion (interquartile range [IQR]), and skewness of the age-frequency distributions (AFDs) for each assemblage. The median ages were compared with the Wilcoxon test, and the shapes were compared with the Kolmogorov-Smirnov (K-S) test, obtaining p values with Monte Carlo simulations due to the small sample size (R package dgof; Arnold and Emerson, 2011). To determine the dynamics of shell loss from the sampled surface sediment layer (here assumed to represent the well-mixed taphonomically active zone [TAZ]) by disintegration and/or burial, we used three models: (1) a one-phase exponential model, defined by a single instantaneous per-individual loss rate λ, (2) a Weibull model with a gradual temporal decline in the loss rate, and (3) a two-phase exponential model that accounts for an abrupt temporal decline from a fast loss λ_1 (initial phase of high disintegration in the TAZ not affected by burial) to a slow loss λ_2 (a function of slower disintegration in the so-called sequestration zone [SZ] and the net rate of shell burial). The SZ can represent patches of sediment with less corrosive conditions within the TAZ or layers immediately below the TAZ; shells from these layers can be still exhumed back into the TAZ by burrowers or by storms, and thus be incorporated into AFDs as measured here. The decline in loss rate from λ_1 to λ_2 occurs at rate τ and can reflect the rate of diagenetic stabilization in the SZ (Tomašových et al., 2014, 2016). The otolith AFD at 10 m showed a drop in skeletal production in the past few centuries and a minimum age of 322 yr (Fig. 2), and the one- and two-phase exponential models were thus adjusted at this site with a parameter setting for the termination of production at 400 yr. We used the Akaike information criterion with correction for small sample sizes (AICc) to identify the best model. We computed the half-lives in the TAZ for the three models according to Tomašových et al. (2016) and the confidence intervals of AFD summary statistics and model parameters with a bootstrapping procedure with 10,000 iterations. We used Spearman rank correlations to assess relations between parameters and median ages and IQRs. All analyses were conducted in the R statistical environment.

RESULTS

The median ages of shell and otolith AFDs were similar within each depth, but they changed strongly and in parallel between depths, with median age equal to ~600–700 yr at 10 m, increasing to ~1400–1500 yr at 30 m, and declining to 13–200 yr at 40 m (Figs. 2 and 3; Table 1). At 10 m, both AFDs were right-skewed, and shape (K-S $D = 0.5$, $p = 0.08$) and median age (Wilcoxon $W = 125$, $p = 0.62$) did not differ between shells and otoliths. The mode of the otolith AFD was at ~500 yr, followed by a sudden

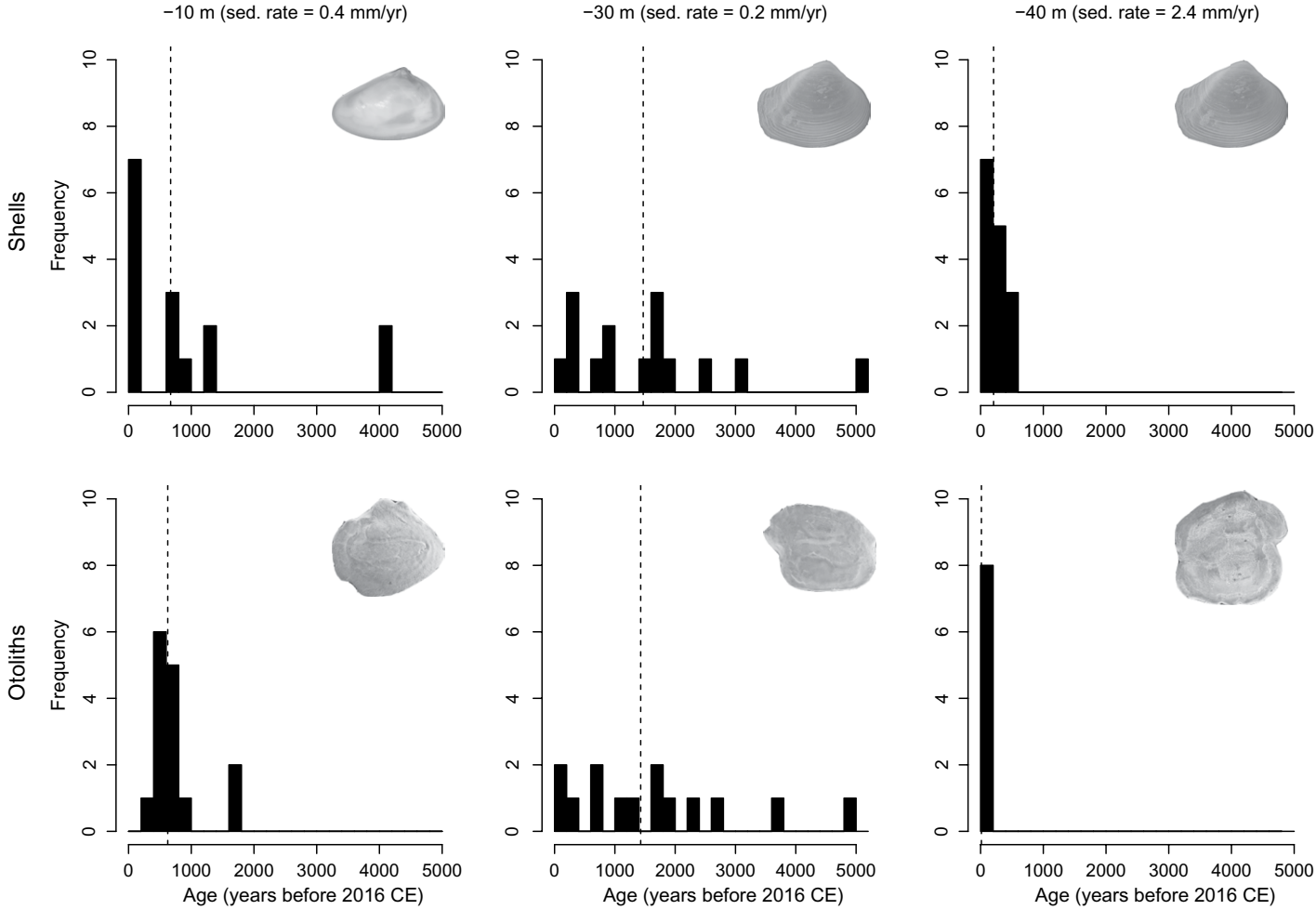

Figure 2. Age-frequency distributions (median probability ages in 200 yr bins) based on calibrated radiocarbon ages for mollusk shells (upper row) and fish otoliths (lower row) across a depth transect off Ashqelon, southern Israel. Dashed lines indicate median ages.

decline in the most recent centuries with a minimum age of 322 yr. This decline in production in the latest few centuries led to a smaller IQR in otoliths (156 yr) than in bivalves (962 yr). At 30 m, the shape (K-S $D = 0.2$, $p = 0.98$), the median ages (Wilcoxon $W = 115.5$, $p = 0.66$), and IQRs (1344 and 1499 yr) did not differ between shells and otoliths. At 40 m, the shape (K-S $D = 0.5$, $p = 0.103$) and the median age (Wilcoxon $W = 33.5$, $p = 0.093$) also did not differ between the two taxa, although differences in IQRs (292 and 18 yr for shells and otoliths, respectively) were slightly larger than at 30 m. To summarize, the differences in median age and IQR between depths exceeded several centuries up to 1000 yr, whereas within-depth differences were less than a few centuries (Fig. 3).

A one-phase exponential model best explained the dynamics of loss of four assemblages, and a two-phase exponential model best explained the other two (Table DR5). However, differences between one- and two-phase models in these four assemblages in AICc were less than six to eight units; i.e., model likelihoods were effectively equal, allowing us to compare assemblages on the basis of the two-phase model (Fig. DR1). Although estimates of λ_1 were variable, they indicated that both shells and otoliths can

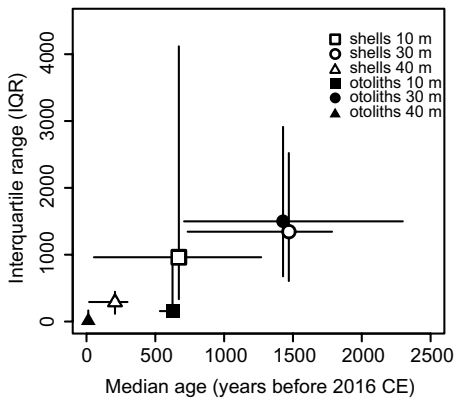

Figure 3. With the exception of interquartile ranges (IQRs) at 10 m, within-depth differences in median age and IQR between shells and otoliths are smaller than between-depth differences off Ashqelon, southern Israel.

TABLE 1. SUMMARY STATISTICS WITH 95% CONFIDENCE INTERVALS FOR THE AGE-FREQUENCY DISTRIBUTIONS OF SHELLS AND OTOLITHS

	−10 m		−30 m		−40 m	
	Shells	Otoliths	Shells	Otoliths	Shells	Otoliths
Number of specimens	15	15	15	14	15	8
Median age (yr)*	671 (54–1269)	625 (533–662)	1470 (735–1784)	1428 (709–2298)	207 (19–298)	13 (7–33)
Age range (yr)	4171 (1225–4186)	1281 (378–300)	4771 (1816–4983)	4753 (2376–4944)	504 (349–504)	167 (16–169)
Interquartile range (IQR) (yr)	962 (334–4118)	156 (72–1042)	1344 (606–2521)	1499 (676–2913)	292 (116–446)	18 (2–166)
Skewness	1.7 (0.15–2.8)	1.5 (−0.4 to 2.9)	1. 0 (−0.3 to 2.0)	0.8 (−0.2 to 1.8)	0.3 (−0 to 1.3)	1.1 (−0.2 to 2.2)

Note: Differences in median age and IQR between depths exceed several centuries, up to 1000 yr, whereas within depths, they are less than a few centuries.
*Ages are in years before 2016 CE (collecting year).

disintegrate rapidly after death, with yearly or decadal half-lives. The estimates of λ_2 showed that through time, both otoliths and shells shifted to half-lives equal to 500–1200 yr at 10 m, to ~1200 yr at 30 m, and to 100–200 yr at 40 m (Fig. DR1).

DISCUSSION

Effect of Burial on AFDs

The major role in shaping the differences in time averaging along the depth gradient was played by the gradients in shell burial rather than by gradients in initial disintegration for two reasons. First, the rate of initial disintegration λ_1 did not correlate with median ages or IQRs (Spearman r for median = –0.37, $p = 0.49$; r for IQR = 0.03, $p = 1$), although it was variable due to constraints from small sample size and temporally variable production. Additionally, the rate of loss λ_2 (which reflects burial and/or later-stage disintegration) correlated negatively with median ages ($r = -0.94$, $p = 0.006$) and IQRs ($r = -0.88$, $p = 0.02$). Second, faster burial at the deepest station was suggested by a sedimentation rate (2.4 mm/yr) that was one order of magnitude greater than at 10 m (0.4 mm/yr) and 30 m (0.2 mm/yr). Medians and IQRs of both shells and otoliths positively correlated with the inverse of sedimentation rates (Spearman r for median = 0.96, $p < 0.002$; r for IQR = 0.84, $p = 0.037$), and λ_2 correlated with sedimentation rate ($r = 0.89$, $p = 0.02$), indicating that this parameter indeed captured the time scale of shell burial below the TAZ, being greater at 10 and 30 m (millennial scale) than at 40 m (centennial scale). In contrast, λ_1 did not vary with sedimentation rate ($r = 0.24$, $p = 0.64$). At 40 m, initial loss was also facilitated by more aggressive pore waters; shells were more brittle than at shallower stations, and none was in pristine condition despite their young age. Accordingly, the two-phase exponential model showed the largest λ_1, also indicating that shells disintegrated at a higher rate at this site. The between-depth differences in sedimentation rates correlated with sediment distribution: Sands at 10 m pass to muddy sands and muds at 30 and 40 m (Table DR1) and thus can reflect stronger bypassing and winnowing of fine-grained sediments driven by wave-induced longshore currents at shallower depths (Stanley, 1989). Sea-level rise did not constrain the maximum age of our studied species along the transect because even the 10 m site was flooded ~8000 yr ago, and the Holocene sea-level rise was limited to 2 m in the past 5000 yr (Sivan et al., 2004). This prevalence of extrinsic factors can be counteracted only by major differences in durability, leading to differences in median ages and IQR by multiple orders of magnitude (Kowalewski et al., 2018).

Consequences for Paleocommunity Studies

Quantification of the time resolution of marine fossil assemblages has been limited so far to primary consumers, such as foraminifera, mollusks, and brachiopods (e.g., Kidwell et al., 2005; Krause et al., 2010; Albano et al., 2016, 2018; Ritter et al., 2017). Fishes are important components of marine trophic webs, and their otoliths preserve species-specific morphology and great abundance in marine and lake sediments (Nolf, 1985) and offer paleobathymetric, paleoclimatic, and other paleoenvironmental information (Agiadi et al., 2018). Comparisons between shells and otoliths are meaningful because of their comparable durability due to similar size, mineralogy, and microstructure. However, otolith postmortem pathways can lead to significant out-of-habitat transport, while infaunal bivalves are more likely to remain buried *in situ* after death. Additionally, the changes in water and nutrient discharge of the Nile River over the entire Holocene (Hassan et al., 2012; Sun et al., 2019) can generate differences in temporal production of groups at different trophic levels. However, our findings indicate that these two intrinsic factors were ultimately negligible and that depth-specific burial pathways independent of taxon identity dominantly contributed to the formation of assemblages with comparable time averaging. Age distributions were not homogenized by cross-shelf transport processes on the high-energy shelf, and these organisms thus spatially and temporally co-occurred in the original living assemblage.

ACKNOWLEDGMENTS

Sampling in Israel was conducted in the framework of the project "Historical ecology of Lessepsian migration" funded by the Austrian Science Fund (FWF) P28983-B29 (principal investigator: Albano). We thank Bella S. Galil for her support throughout the planning and running of the Lessepsian project, and Erin Dillon for discussions. Otolith dating was supported by research grant PA-RG201803 from the Palaeontological Association (UK) to Agiadi. Shell dating was supported by a grant by the University of Vienna (Austria) to Zuschin. Tomašových was supported by the Slovak Research and Development Agency (APVV17–0555). Jan Steger, Danae Thivaiou, Katherine Whitacre, and Jordon Bright prepared samples, which were analyzed for radiocarbon at the University of California–Irvine Keck Accelerator Mass Spectrometer Laboratory. Jan Päßler analyzed the sediment granulometry. Itay Katzman and the crew of the *Mediterranean Explorer* vessel helped throughout the field work. Three anonymous reviewers provided useful comments on the initial manuscript.

REFERENCES CITED

Agiadi, K., Girone, A., Koskeridou, E., Moissette, P., Cornée, J.-J., and Quillévéré, F., 2018, Pleistocene marine fish invasions and paleoenvironmental reconstructions in the eastern Mediterranean: Quaternary Science Reviews, v. 196, p. 80–99, https://doi.org/10.1016/j.quascirev.2018.07.037.

Albano, P.G., Filippova, N., Steger, J., Kaufman, D.S., Tomašových, A., Stachowitsch, M., and Zuschin, M., 2016, Oil platforms in the Persian (Arabian) Gulf: Living and death assemblages reveal no effects: Continental Shelf Research, v. 121, p. 21–34, https://doi.org/10.1016/j.csr.2015.12.007.

Albano, P.G., Gallmetzer, I., Haselmair, A., Tomašových, A., Stachowitsch, M., and Zuschin, M., 2018, Historical ecology of a biological invasion: The interplay of eutrophication and pollution determines time lags in establishment and detection: Biological Invasions, v. 20, p. 1417–1430, https://doi.org/10.1007/s10530-017-1634-7.

Arnold, T.B., and Emerson, J.W., 2011, Nonparametric goodness-of-fit tests for discrete null distributions: The R Journal, v. 3, p. 34, https://doi.org/10.32614/RJ-2011-016.

Avnaim-Katav, S., Hyams-Kaphzan, O., Milker, Y., and Almogi-Labin, A., 2015, Bathymetric zonation of modern shelf benthic foraminifera in the Levantine Basin, eastern Mediterranean Sea: Journal of Sea Research, v. 99, p. 97–106, https://doi.org/10.1016/j.seares.2015.02.006.

Best, M.M.R., Ku, T.C.W., Kidwell, S.M., and Walter, L.M., 2007, Carbonate preservation in shallow marine environments: Unexpected role of tropical siliciclastics: The Journal of Geology, v. 115, p. 437–456, https://doi.org/10.1086/518051.

Bush, S.L., Santos, G.M., Xu, X., Southon, J.R., Thiagarajan, N., Hines, S.K., and Adkins, J.F., 2013, Simple, rapid, and cost effective: A screening method for ^{14}C analysis of small carbonate samples: Radiocarbon, v. 55, p. 631–640, https://doi.org/10.1017/S0033822200057787.

Degens, E.T., Deuser, W.G., and Haedrich, R.L., 1969, Molecular structure and composition of fish otoliths: Marine Biology, v. 2, p. 105–113, https://doi.org/10.1007/BF00347005.

Elder, R.L., and Smith, G.R., 1988, Fish taphonomy and environmental inference in paleolimnology: Palaeogeography, Palaeoclimatology, Palaeoecology, v. 62, p. 577–592, https://doi.org/10.1016/0031-0182(88)90072-7.

Gallmetzer, I., Haselmair, A., Tomašových, A., Mautner, A.-K., Schnedl, S.-M., Cassin, D., Zonta, R., and Zuschin, M., 2019, Tracing origin and collapse of Holocene benthic baseline communities in the northern Adriatic Sea: Palaios, v. 34, p. 121–145, https://doi.org/10.2110/palo.2018.068.

Golik, A., 1993, Indirect evidence for sediment transport on the continental shelf off Israel: GeoMarine Letters, v. 13, p. 159–164, https://doi.org/10.1007/BF01593189.

Goodman-Tchernov, B.N., Dey, H.W., Reinhardt, E.G., McCoy, F., and Mart, Y., 2009, Tsunami waves generated by the Santorini eruption reached Eastern Mediterranean shores: Geology, v. 37, p. 943–946, https://doi.org/10.1130/G25704A.1.

Hassan, F.A., Hamdan, M.A., Flower, R.J., and Keatings, K., 2012, The oxygen and carbon isotopic records in Holocene freshwater mollusc shells from the Faiyum paleolakes, Egypt: Their paleoenvironmental and paleoclimatic implications: Quaternary International, v. 266, p. 175–187, https://doi.org/10.1016/j.quaint.2011.11.024.

Hyams-Kaphzan, O., Almogi-Labin, A., Sivan, D., and Benjamini, C., 2008, Benthic foraminifera assemblage change along the southeastern Mediterranean inner shelf due to fall-off of Nile-derived siliciclastics: Neues Jahrbuch für Geologie und Paläontologie, Abhandlungen, v. 248, p. 315–344, https://doi.org/10.1127/0077-7749/2008/0248-0315.

Inman, D.L., and Jenkins, S.A., 1984, The Nile littoral cell and man's impact on the coastal zone of the southeastern Mediterranean: Coastal Engineering Proceedings, v. 1, p. 1600–1617, https://doi.org/10.9753/icce.v19.109.

Kidwell, S.M., 2013, Time averaging and fidelity of modern death assemblages: Building a taphonomic foundation for conservation palaeobiology: Palaeontology, v. 56, p. 487–522, https://doi.org/10.1111/pala.12042.

Kidwell, S.M., Best, M.M.R., and Kaufman, D.S., 2005, Taphonomic trade-offs in tropical marine death assemblages: Differential time averaging, shell loss, and probable bias in siliciclastic vs. carbonate facies: Geology, v. 33, p. 729–732, https://doi.org/10.1130/G21607.1.

Kosnik, M.A., Hua, Q., Jacobsen, G.E., Kaufman, D.S., and Wüst, R.A., 2007, Sediment mixing and stratigraphic disorder revealed by the age-structure of *Tellina* shells in Great Barrier Reef sediment: Geology, v. 35, p. 811–814, https://doi.org/10.1130/G23722A.1.

Kosnik, M.A., Hua, Q., Kaufman, D.S., and Wüst, R.A., 2009, Taphonomic bias and time averaging in tropical molluscan death assemblages: Differential shell half-lives in Great Barrier Reef sediment: Paleobiology, v. 35, p. 565–586, https://doi.org/10.1666/0094-8373-35.4.565.

Kosnik, M.A., Kaufman, D.S., and Hua, Q., 2013, Radiocarbon-calibrated multiple amino acid geochronology of Holocene molluscs from Bramble and Rib Reefs (Great Barrier Reef, Australia): Quaternary Geochronology, v. 16, p. 73–86, https://doi.org/10.1016/j.quageo.2012.04.024.

Kowalewski, M., 1996, Time averaging, overcompleteness, and the geological record: The Journal of Geology, v. 104, p. 317–326, https://doi.org/10.1086/629827.

Kowalewski, M., Casebolt, S., Hua, Q., Whitacre, K.E., Kaufman, D.S., and Kosnik, M.A., 2018, One fossil record, multiple time resolutions: Disparate time averaging of echinoids and mollusks on a Holocene carbonate platform: Geology, v. 46, p. 51–54, https://doi.org/10.1130/G39789.1.

Krause, R.A., Barbour, S.L., Kowalewski, M., Kaufman, D.S., Romanek, C.S., Simões, M.G., and Wehmiller, J.F., 2010, Quantitative comparisons and models of time averaging in bivalve and brachiopod shell accumulations: Paleobiology, v. 36, p. 428–452, https://doi.org/10.1666/08072.1.

Lyons, S.K., et al., 2016, Holocene shifts in the assembly of plant and animal communities implicate human impacts: Nature, v. 529, p. 80–83, https://doi.org/10.1038/nature16447.

Nolf, D., 1985, Otolithi piscium, *in* Schlutze, H.P., ed., Handbook of Paleoichthyology, Vol. 10: Stuttgart, Germany, G. Fischer Verlag, p. 145.

Nolf, D., 1995, Studies on otolith fossils: The state of the art, *in* Secor, D.H., et al., eds., Recent Developments in Fish Otolith Research: Columbia, South Carolina, University of South Carolina Press, p. 513–544.

Ritter, M.D.N., Erthal, F., Kosnik, M.A., Coimbra, J.C., and Kaufman, D.S., 2017, Spatial variation in the temporal resolution of subtropical shallow-water molluscan death assemblages: Palaios, v. 32, p. 572–583, https://doi.org/10.2110/palo.2017.003.

Roopnarine, P.D., and Angielczyk, K.D., 2015, Community stability and selective extinction during the Permian-Triassic mass extinction: Science, v. 350, p. 90–93, https://doi.org/10.1126/science.aab1371.

Sivan, D., Lambeck, K., Toueg, R., Raban, A., Porath, Y., and Shirman, B., 2004, Ancient coastal wells of Caesarea Maritima, Israel, an indicator for relative sea level changes during the last 2000 years: Earth and Planetary Science Letters, v. 222, p. 315–330, https://doi.org/10.1016/j.epsl.2004.02.007.

Stanley, D.J., 1989, Sediment transport on the coast and shelf between the Nile Delta and Israeli margin as determined by heavy minerals: Journal of Coastal Research, v. 5, p. 813–828.

Sun, Q., Liu, Y., Salem, A., Marks, L., Welc, F., Ma, F., Zhang, W., Chen, J., Jiang, J., and Chen, Z., 2019, Climate-induced discharge variations of the Nile during the Holocene: Evidence from the sediment provenance of Faiyum Basin, north Egypt: Global and Planetary Change, v. 172, p. 200–210, https://doi.org/10.1016/j.gloplacha.2018.10.005.

Tomašových, A., Kidwell, S.M., Barber, R.F., and Kaufman, D.S., 2014, Long-term accumulation of carbonate shells reflects a 100-fold drop in loss rate: Geology, v. 42, p. 819–822, https://doi.org/10.1130/G35694.1.

Tomašových, A., Kidwell, S.M., and Barber, R.F., 2016, Inferring skeletal production from time-averaged assemblages: Skeletal loss pulls the timing of production pulses towards the modern period: Paleobiology, v. 42, p. 54–76, https://doi.org/10.1017/pab.2015.30.

Tomašových, A., Gallmetzer, I., Haselmair, A., Kaufman, D.S., Mavrič, B., and Zuschin, M., 2019, A decline in molluscan carbonate production driven by the loss of vegetated habitats encoded in the Holocene sedimentary record of the Gulf of Trieste: Sedimentology, v. 66, p. 781–807, https://doi.org/10.1111/sed.12516.

Villéger, S., Novack-Gottshall, P.M., and Mouillot, D., 2011, The multidimensionality of the niche reveals functional diversity changes in benthic marine biotas across geological time: Ecology Letters, v. 14, p. 561–568, https://doi.org/10.1111/j.1461-0248.2011.01618.x.

Printed in USA